

Is a Circular Rydberg Atom Stable in a Vanishing Electric Field?

M. Gross and J. Liang

Laboratoire de Spectroscopie Hertzienne de l'Ecole Normale Supérieure, 75231 Paris Cedex 05, France

(Received 19 September 1986)

It is shown both experimentally and theoretically that a Rydberg circular atom keeps its maximum momentum only if it is submitted to a nonzero static electric field whose direction is constant or slowly varying. The minimum characteristic time of the field-allowed rotation is determined. The implications of this effect for a future high-resolution microwave spectroscopy experiment on circular Rydberg atoms is discussed.

PACS numbers: 31.60.+b, 32.60.+i

High-angular-momentum Rydberg states of alkali-metal atoms have very peculiar properties with respect to static electric fields. For an orbital quantum number l larger than a few units, the various l levels of an n manifold (where n is the principal quantum number) are quasidegenerate: The energy shift between consecutive n, l and $n, l+1$ states is proportional to $n^{-3}l^{-6}$,¹ and becomes exceedingly small. The system is thus hydrogenic. A very low static electric field is able to couple strongly levels with different l values, and Stark shifts linear with respect to the field are observed. The static electric field eigenstates are the n , m , and n_1 states of the parabolic Stark basis² with the electric field direction as a quantization axis.

Most of the high-angular-momentum³ and circular-state Rydberg experiments⁴⁻⁶ have been performed in experimental situations where a constant-direction Stark field is applied to the atoms. This feature is in fact fundamental to remove the l degeneracy and to provide stability to the high-angular-momentum atoms.

In this Letter, we will discuss both experimentally and theoretically how circular atoms evolve when the applied Stark field rotates. We will see that the atomic system state is then able to move in the n -manifold n^2 -dimensional space, changing both l and m (in the spherical basis), or m and n_1 (in the parabolic one). This physical effect manifests itself when one tries to cancel the applied electric field. In this case, there is no privileged axis and no reason for the system to keep its initial orientation. The stray fields, whose order of magnitude is typically 10 mV/cm to 1 V/cm, strongly couple the levels of the n manifold, and are able to change both the orientation (m) and the eccentricity (l) of the valence-electron orbit (the field direction generally varies with space and the moving atom sees a rotating field). The circular atom then loses its circular character.

The electric field effect on high-angular-momentum atoms can be studied by use of a simple classical model (n , l , and m are all large). The motion of the Rydberg electron in an external field \mathbf{F} is⁷

$$d(\mathbf{L} \pm \mathbf{A})/dt = \pm \omega_S \times (\mathbf{L} \pm \mathbf{A}). \quad (1)$$

\mathbf{L} and \mathbf{A} are the time averages of the electron orbital momentum: $\mathbf{r} \times \mathbf{p}$, and the Runge-Lenz vector⁸

$$m^{-1}(\mathbf{r} \times \mathbf{p}) \times \mathbf{p} + (q^2/4\pi\epsilon_0)\mathbf{r}/r.$$

\mathbf{L} , \mathbf{A} , and the electric field \mathbf{F} are supposed to vary slowly with respect to the electron orbital motion (secular approximation). ω_S is the hydrogen Stark frequency:

$$\omega_S = \frac{3}{2}n(4\pi\epsilon_0 a_0/m)^{1/2}E, \quad (2)$$

where a_0 is the hydrogen Bohr radius and m is the electron mass. For $n=25$ and $|\mathbf{E}|=1$ V/cm, Eq. (2) yields to $\omega_S=2\pi \times 4.8 \times 10^7$ rad/s.

Initially, the atomic system is prepared in a circular state: $\mathbf{A}=0$, $|\mathbf{L}|=(n-1)\hbar$, with an electric field \mathbf{F} and the angular momentum \mathbf{L} both oriented in the same \mathbf{u}_z direction. This last assumption is automatically fulfilled when circular states are prepared by the adiabatic microwave transfer method.⁴ Figure 1 presents (solid line) for various values of ω_S/ω_R the \mathbf{L} motion in the

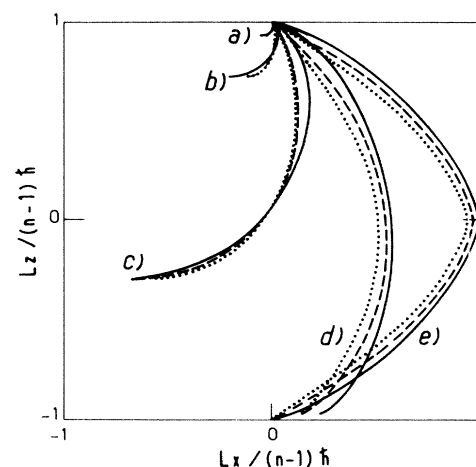


FIG. 1. Trajectories of the \mathbf{L} motion in the \mathbf{u}_x , \mathbf{u}_z plane when the electric field rotates [Eq. (3)]. Curves a , b , c , d , and e correspond to $\omega_S/\omega_R=0.2, 0.4, 1, 2$, and 4 , respectively. The dotted lines correspond to $n=10$, the dashed lines to $n=20$, and the solid lines to the classical evolution $n=\infty$.

u_x, u_z plane, when \mathbf{F} is rotated from $+\mathbf{u}_z$ to $-\mathbf{u}_z$ in a time π/ω_R ,

$$\mathbf{F} = F[\cos(\omega_R t)\mathbf{u}_z + \sin(\omega_R t)\mathbf{u}_x]. \quad (3)$$

Note that the \mathbf{L} projection in the u_y direction is always zero.

If the field is slowly rotated at a frequency ω_R much lower than ω_S , Eq. (1) shows that the atomic system adiabatically follows the field. \mathbf{L} keeps its maximum amplitude $(n-1)\hbar$ and remains oriented along the field. \mathbf{A} remains zero (adiabatic approximation). This case is illustrated in Fig. 1, curve *e*. If, on the contrary, the field rotation is fast, $\omega_R \gg \omega_S$, the atomic system does not evolve during the rotation and \mathbf{L} remains oriented along u_z . This sudden-approximation regime corresponds to Fig. 1, curve *a*. In both cases, with a quantization axis along u_z , the system is still, after rotation of the field, in a circular state, oriented either in the $-\mathbf{u}_z$ direction ($l = -m = n-1$) for the adiabatic $\omega_R \ll \omega_S$ case, or in the $+\mathbf{u}_z$ direction ($l = +m = n-1$) for the $\omega_S \gg \omega_R$ case.

In all the intermediate cases (see Fig. 1, curve *c*), the atomic system evolves during the rotation of the field, but is unable to follow it adiabatically. The final state is complex. The \mathbf{L} amplitude is no longer maximum: $l < (n-1)$, \mathbf{A} is nonvanishing, and both \mathbf{L} and \mathbf{A} are no longer oriented in the u_z direction.

In order to check the validity of this classical model, we have computed and presented in Fig. 1 the quantum evolution of the atomic system, for $n=10$ (dashed lines) and $n=20$ (dotted lines), choosing the electric field amplitude so that the ratios ω_S/ω_R have the same values as for the classical model calculation (solid lines). The computation is done by direct integration of the Schrödinger equation in the spherical n, l , and m basis. The electric field \mathbf{F} is considered as a classical perturbation varying in time, in the dipolar hydrogenic Hamiltonian: $H = \mathbf{E} \cdot \mathbf{D}$. As n is large, the evolutions of the quantum average expected values $\langle \mathbf{L} \rangle$ of \mathbf{L} are very close to the corresponding classical ones. Note that here, as n is not infinite, $\langle \mathbf{L} \rangle$ is not strictly in the u_x, u_z plane: $\langle L_y \rangle \neq 0$.

The experimental setup used to study these effects is very similar to the one used by our group in a previous experiment.⁶ The $n=25$ circular atoms of lithium are similarly produced by the adiabatic microwave transfer method from the parabolic $n=25, m=2, n_1=0$ state, prepared by three YAlG (yttrium aluminum garnet)-pumped dye-laser steps at 6708 Å ($2s \rightarrow 2p$), 6104 Å ($2p \rightarrow 3d$), and 8313 Å ($3d \rightarrow n=25, m, n_1$), respectively. A 2.2-kV/cm ionizing pulsed voltage, rising in 10 μs [see Fig. 2(a), feature 3], is applied across the 6-mm-spaced ionizing plane condenser, and the ionization current is recorded.

In order to make the atoms experience a rotating low Stark field, the ionization condenser has been modified.

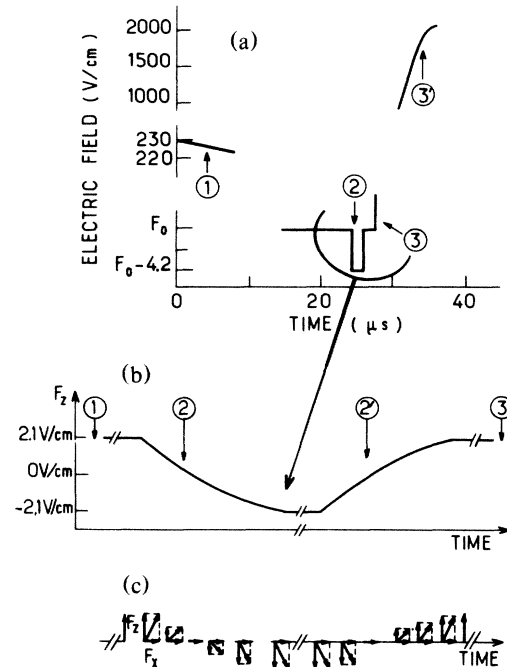


FIG. 2. (a) Vertical component of the electric field as a function of time seen by the $V=1750$ m/s detected atoms. (b) Detailed view of the mixing pulse. (c) Schematic view of the field rotation.

Its forward part (with respect to the beam) is made of two series of thirteen copper printed-circuit strips orthogonally oriented with respect to the beam axis u_x . A 4.03-V voltage (three mercury oxide watch batteries) is regularly distributed along both series of $\frac{1}{10}$ -in. periodically spaced strips by a resistive network. This produces a 1.33-V/cm electric field along the u_x direction. Applying a small, experimentally controlled V_M mixing voltage ($-2.5 \text{ V} < V_M < +2.5 \text{ V}$) across the condenser enables us to vary both the electric field \mathbf{F} vertical component F_z and direction \mathbf{F}/F .

In Fig. 2, F_z is plotted as a function of space and/or time along the atomic beam for the 1750-m/s velocity-detected atoms. Feature 1 is the large, slowly time-varying field used for preparation of the circular states. Feature 2 is the mixing pulse and features 3 and 3' the ionizing pulse.

The studied effect takes place at the very time when the field rotates, i.e., when F_z reverses sign. Depending on the dc component F_0 of the field F_z applied across the condenser, this happens either during the mixing pulse (feature 2) or at the very beginning of the ionizing pulse (feature 3).

Figure 2(b) shows, with more detail, for $F_0=0$, how the vertical component F_z reverses sign during the falling (feature 2) and the rising (feature 2') edges of the mixing pulse. Figure 2(c) shows how the corresponding field

direction varies.

Figure 3 shows the time-resolved ionization signal obtained under various conditions. For Fig. 3, curve *a*, the 9.2-GHz microwave used to prepare the circular states is switched off. Figure 3, curve *b*, shows the $n=25$ circular state signature. The largest peak corresponds to the $n=25$ circular state itself. The two smaller side peaks can be assigned to the $n=24$ and $n=26$ adjacent circular states populated by blackbody radiation transfer from the $n=25$ circular state. Curves *a* and *b* in Fig. 3 are very similar to curves *a* and *b* in Fig. 2 of Ref. 6 except for the time origin and sign of the presented signal (which appears on a dark background). Curves *c-g* in Fig. 3 show the ionizing signals in the presence of a mixing pulse going from $F_z = 2.1$ V/cm to $F_z = -2.1$ V/cm and back for different values of the falling and rising slew rate.

Using the direct Schrödinger integration technique described above, we have computed the normalized population of the $n=25$ oriented circular state, after the mixing pulse. One gets 0.99, 0.86, 0.82, and 0.12, and 0.0 for the mixing-pulse field velocities of Fig. 3, curves *c-g*, respectively. When this quantity is very close to 1 (0.99), no significant change, compared to the circular case (Fig. 3, curve *b*), is observed on the ionizing signal

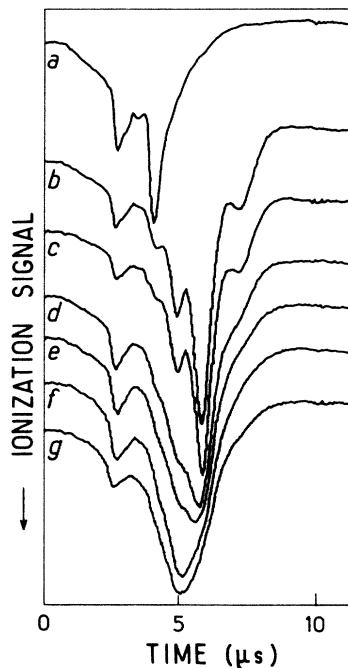


FIG. 3. Field ionization signals with a 1.33-V/cm horizontal field. Curve *a*: initial $n=25$, $m=2$, $n_1=0$ state. Curve *b*: circular $n=25$, $m=24$ state. Curves *c*, *d*, *e*, *f*, and *g*: circular states in the presence of a mixing pulse whose falling and rising slew rates are respectively -120 and $+100$ (curve *c*), -220 and $+140$ (curve *d*), -270 and $+150$ (curve *e*), -330 and $+160$ (curve *f*), and -700 and $+200$ V/cm $\cdot\mu$ s (curve *g*).

(Fig. 3, curve *c*). When it is smaller than 1, remaining of the order of 1 (0.86, 0.82), ionization takes place for lower voltage (shorter time), but the high-field narrow circular peak is still present (Fig. 3, curves *d* and *e*). When it is much smaller than 1 (0.12, 0), the circular peak disappears (Fig. 3, curves *f* and *g*). One observes, upon the increase of the field velocity in Fig. 3, curves *d-g*, a broadening and a shift of the ionizing peak to shorter time and lower field. This corresponds to a population transfer from the $m=24$ circular state to lower angular momentum states $m < 24$ which ionize in lower fields. As a large number of m, l sublevels are then populated (this can be checked by integration of the Schrödinger equation), ionization takes place on a larger field domain.

A control experiment has been performed by reversal of the direction of the horizontal field. No significant change has been observed. The mixing effect has also been seen in the horizontal parasitic field present without the batteries. It corresponds to a 0.3-V/cm horizontal field.

A last experiment has been made in the 0.3-V/cm parasitic field, without application of any mixing voltage. Depending on the value of the dc field $F_0 = \pm 5$ V/cm, the electric field rotates or not at the very beginning of the ionizing pulse. When this pulse rises rather slowly (Fig. 4, curve *a*), the ionizing signal corresponding to a

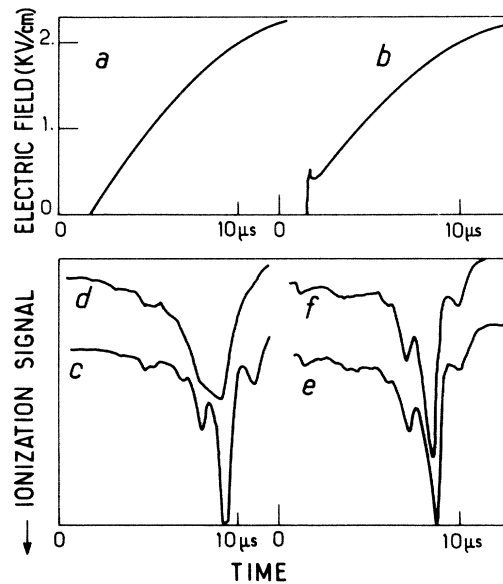


FIG. 4. Curves *a* and *b*: slow- and fast-rising ionizing pulses. Curves *c*, *d*, *e*, and *f*: field ionization signal with a 0.3-V/cm horizontal field, and without mixing pulse. Curves *c* and *d*: nonrotating and rotating signals ($F_0 = +5$ and -5 V/cm) corresponding to the slow-rising (225 V/cm $\cdot\mu$ s) pulse of curve *a*. Curves *e* and *f*: nonrotating and rotating signals corresponding to the fast-rising (4×10^4 V/cm $\cdot\mu$ s) pulse of curve *b*.

rotating field (Fig. 4, curve *d*) is very different from the nonrotating one (Fig. 4, curve *c*). This corresponds to the previously studied mixing effect. When the field rises very fast (Fig. 4, curve *b*), the atomic system has no time to evolve during the field rotation and, after it, is still in a circular state (whose helicity has been reversed with the quantization axis). The rotating and nonrotating ionizing signals have then the same shape (Fig. 4, curves *f* and *e*, respectively). This corresponds to the sudden approximation regime.

An electric field acting on the high-angular-momentum Rydberg atom is a major parameter which must be controlled. Its effect can be analyzed simply by the classical model [Eq. (1)]. This model predicts, for example, that a circular-atom orbit plane which is initially orthogonal to the field tends to follow adiabatically the field direction. When the field rotates, an unwanted nonadiabatic *m*-mixing coupling effect can be avoided by use of higher fields.⁵

Careful control of the electric field may allow the movement of the atom state in the *n*-multiplicity two-dimensional space (*m, l* or *m, n₁*). Nutation of *l* is expected if an initially circular atom is submitted to a constant field parallel to the initial circular orbit plane. This *l* nutation (inside the *n* multiplicity) is similar to the *m*-Zeeman nutation (inside the *n, l* multiplicity) in a magnetic field orthogonal to the quantization axis.

To make circular atoms stable, it is thus necessary to apply a *nonvanishing* electric field, *orthogonally oriented* with respect to the orbit plane, whose *direction is constant* or slowly varying ($\omega_S \gg \omega_R$). These three conditions must be fulfilled in any experiment where long-

lived circular atoms are wanted. Circular Rydberg-atom high-resolution microwave spectroscopy experiments can be done in such a way. A low applied constant field $F \sim 30$ mV is large enough to overcome stray fields in a typical microwave cavity environment, providing the necessary quantization axis ($\omega_S \sim 1.4$ MHz for $n = 25$) without modifying the transition frequency (the $25 \rightarrow 24$ circular-circular 447-GHz microwave transition is shifted by ~ 8 Hz).⁶

This work has been performed at the Ecole Normale Supérieure in the Laboratoire de Spectroscopie Hertzienne, Unité No. 18, associé au Centre National de la Recherche Scientifique. One of us (J.L.) acknowledges support from the allocation de Recherches de la Fondation Hugot du Collège de France.

¹R. Freeman and D. Kleppner, Phys. Rev. A **14**, 1614 (1976); C. Fabre, Ann. Phys. (Paris) **7**, 5 (1982).

²H. A. Bethe and E. E. Salpeter, *Quantum Mechanics of One- and Two-Electron Atoms* (Springer-Verlag, Berlin, 1957).

³R. G. Rolfes, D. B. Smith, and K. B. McAdam, J. Phys. B **16**, L535 (1983).

⁴R. G. Hulet and D. Kleppner, Phys. Rev. Lett. **51**, 1430 (1983).

⁵R. G. Hulet, E. S. Hilfer, and D. Kleppner, Phys. Rev. Lett. **55**, 2137 (1985).

⁶J. Liang, M. Gross, P. Goy, and S. Haroche, Phys. Rev. A **33**, 4437 (1986).

⁷C. Chardonnet, Thèse 3ème cycle, Université Paris VI, 1983 (unpublished).

⁸W. Pauli, Z. Phys. **36**, 336 (1926).